Does Location of BODIPY Ring Functionalization Affect Electron Transfer Properties? Studies on α, β and meso-functionalized BODIPY Derived Donor-Acceptor Dyads and Triads

Jivan S. Shinde,[a‡] Michael B. Thomas,[b‡] Madhurima Poddar,[a] Rajneesh Misra,*[,a] Francis D'Souza*[,b]

a. Department of Chemistry, Indian Institute of Technology, Indore 453552, India.

E-mail: rajneeshmisra@iiti.ac.in

b. Department of Chemistry, University of North Texas, 1155 Union Circle, #305070, 76203-5017, Denton, TX, USA.E-mail: Francis.DSouza@UNT.edu

ABSTRACT: The effect of positioning an electron donor, ferrocene (Fc), and a charge transfer complex, Fc-tetracyanobutadine (TCBD) at different locations of the BF_2-chelated dipyrromethene (BODIPY) ring in governing excited state charge separation is reported. For this, BODIPY was functionalized at the meso, α-, or β-pyrrole positions with an acetylene spacer carrying either a Fc or a Fc-TBCD charge transfer complex. Among the *meso*-, *α*- or *β*-pyrrole derivatized BODIPYs, $E_{0,0}$ and Stokes shift were found to depend upon the position of BODIPY ring functionalization, independent of polarity. The Stokes shift followed the order *β* > *meso* > *α*- substitution for a given series of BODIPY derivatives while the $E_{0,0}$ followed the order *meso* > *α*- > *β*-substitution. Using a combination of Pd-catalyzed Sonogashira cross-coupling reaction and [2+2] cycloaddition–retroelectrocyclization reaction involving tetracyano ethylene to introduce TCBD between the BODIPY and Fc entities was designed and followed. From the newly established energy level diagram using spectral, computational, and electrochemical results, formation of $BODIPY^{\bullet-}$-Fc^+ in the case of dyads, and $(BODIPY\text{-}TCBD)^{\bullet-}$-$Fc^+$ in the case of triads from $^1BODIPY^*$ was possible to arrive. Femtosecond transient absorption studies followed by data analysis through target analysis confirmed this to be the case. Importantly, in the case of BODIPY-Fc dyads, α-pyrrole-functionalized derivatives performed better in terms of stabilizing the charge separated state while in the case of BODIPY-TCBD-Fc triads, stabilization of $(BODIPY\text{-}TCBD)^{\bullet-}$-$Fc^+$ for β-pyrrole functionalized derivative was better. The present findings on spectral and photochemical properties in differently functionalized BODIPYs are important not only for light energy harvesting but also in designing the next generation of BODIPY based fluorescence probes and sensors.

INTRODUCTION

Establishing structure-function relations in light induced charge separation processes in synthetic donor-acceptor conjugates is not only important to further our understanding of natural photosynthesis[1-2] but is also vital for solar energy harvesting and building optoelectronic devices.[3-26] In this context, harvesting sunlight into chemical energy by an artificial photosynthetic approach is considered one of the possible solutions to fulfil the ever increasing global energy needs without significantly affecting the environment.[1-2] For this, a wide variety of artificial photosynthetic donor-acceptor conjugates have been designed and synthesized; some of these systems have shown to be capable of both wide-band capture of solar photons and the ability to use the absorbed energy to generate charge-separated states of appreciable energy.[3-13] Using elegant synthetic chemistry, it has been possible to fine-tune the light capture and conversion efficiency to a desired value by altering the D/A units, their relative distance, and the π-linker connecting them.[3-26]

BODIPYs (see Figure 1 for structure) have gained much attention in recent years as building blocks of artificial photosynthetic systems, sensors and probes.[29-32] BODIPYs exhibit high absorption coefficients, high fluorescence quantum yields, and tunable redox potentials.[33-36] Their electronic and photonic properties can be tuned by a proper choice of electron rich/deficient addends and by performing substitution at different positions of the BODIPY macrocycle.[29-32,33-36] These features have made BODIPY an attractive

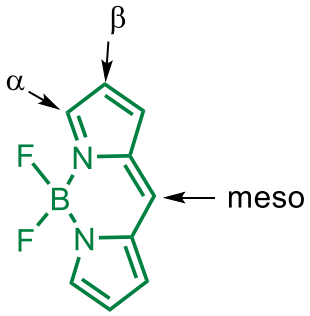

Figure 1. BODIPY skeleton and naming of ring carbons.

fluorophore as its absorption can be extended over a wide spectral range. In recent years, our groups have explored various antenna-donor-acceptor model compounds possessing BODIPY as one of the active components.[18-26,37-38]In the majority of the studies where BODIPY formed part of the donor-acceptor system, the functionalization was carried out at the *meso*-position.[18-26,29-32,33-36] Only a handful of studies utilized the pyrrole α and β positions.[29-38] Importantly, although

substitution effect on absorption and fluorescence properties as a function of different location of BODIPY ring has been performed,[35] no systematic study has been reported on the substitution effects of different locations on the BODIPY ring on their electron transfer properties. In the present study, we have undertaken a task where BODIPY has been functionalized at the *meso*-, α-, and β-pyrrole positions to visualize its effects on the spectral and electrochemical properties with acetylene (**1–3** in Figure 2) and bis-acetylene (**4–6**) π-extenders. Further, using the Pd-catalyzed Sonogashira cross-

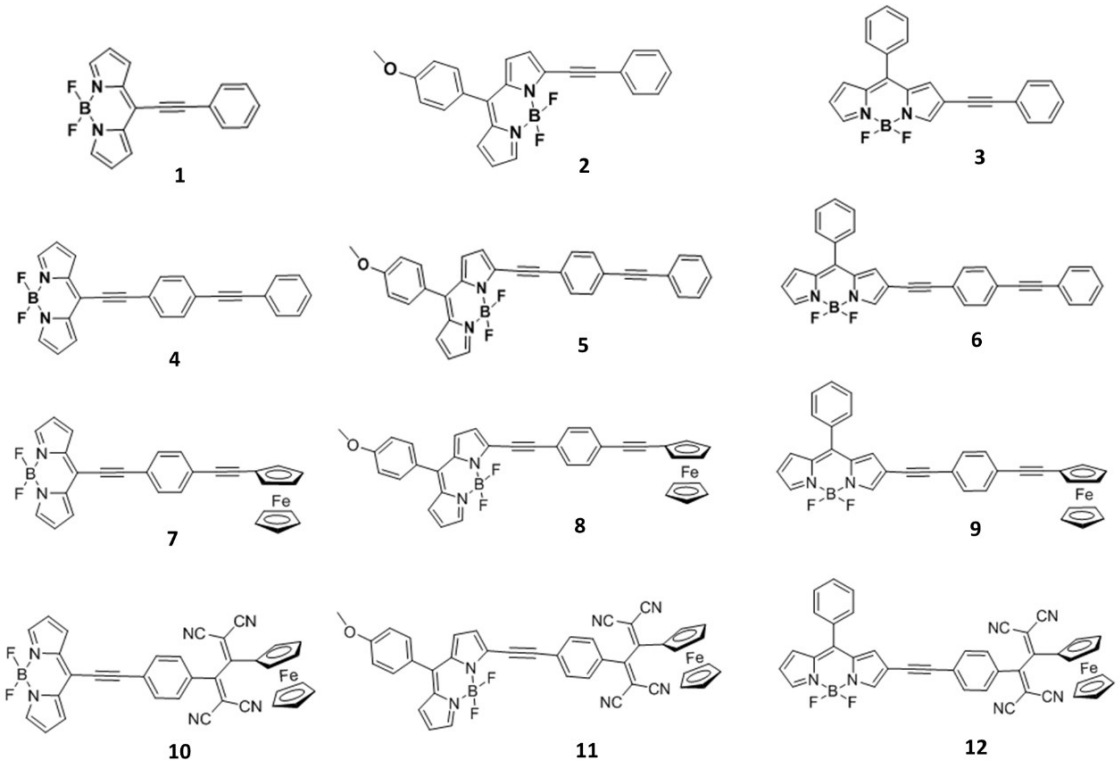

Figure 2. Structures of the differently functionalized BODIPYs, BODIPY-ferrocene dyads, and BODIPY-TCBD-ferrocene (BODIPY-TCBD-Fc) triads charge transfer systems.

coupling reaction, the terminal phenyl ring in **4–6** have been replaced with an electron donor, ferrocene, to result in the BODIPY-Fc dyads, **7–9**. Finally, with the help of a [2+2] cycloaddition–retroelectrocyclization reaction,[39] an electron acceptor entity, tetracyanobuta-1,3-diene (TCBD), has been introduced between the BODIPY and ferrocene entities of dyads **7–9** to result BODIPY-TCBD-Fc charge transfer complexes, **10–12**. Earlier, TCBD has been covalently linked to electroactive units such as anilines, porphyrins, corannulenes, phthalocyanines subphthalocyanine, or BODIPY and others sensitizers.[40-54] In majority of these TCBD-based charge transfer complexes,

excited state charge transfer has been observed. As part of the investigation, the ground and excited state processes in the newly synthesized systems have been systematically studied to visualize BODIPY substitution effects in governing the ground and excited state interactions in polar benzonitrile. Effect of location of BODIPY ring functionalization in governing photoinduced charge separation, has been demonstrated in these dyads and triads from studies involving the pump-probe spectroscopic technique.

RESULTS AND DISCUSSION

Synthesis

The synthetic methodology developed for differently substituted BODIPY systems is shown in Schemes 1 and S1, while the synthetic details are given in SI. The ferrocenyl substituted BODIPYs **7**, **8**, and **9** were synthesized by the Sonogashira cross-coupling reaction of *meso* (8-chloro), *α*-bromo, and *β*-iodo BODIPYs with 1-ethynyl-4-(ethynylferrocene)benzene, respectively. The TCBD bridged BODIPYs **10**, **11**, and **12** were synthesized by the [2+2] cycloaddition–retroelectrocyclization reaction of ferrocenyl substituted BODIPYs **7**, **8**, and **9** with tetracyanoethene (TCNE), respectively (Schemes 1 and S1).

The precursors α-bromo BODIPY, β-iodo BODIPY and 8-chloro BODIPY were synthesized by reported procedures (Scheme S1).[55-57] The α-ferrocenyl substituted BODIPY **8** was synthesized by the Pd-catalyzed Sonogashira cross-coupling reaction of α-bromo BODIPY with 1-ethynyl-4-(ethynylferrocene)benzene (1 equiv.) in THF solvent at 60 °C in 81% yield. Similarly the β-ferrocenyl substituted BODIPY **9** was synthesized by Sonogashira cross-coupling reaction of β-iodo BODIPY with 1-ethynyl-4-(ethynylferrocene) benzene (1 equiv.) in THF solvent by using base, di-isopropylethylamine (DIPEA), at 60 °C in 86% yield.[55-57] The 1,1,4,4-tetracyanobuta-1,3-diene (TCBD) substituted BODIPYs (**11** and **12**) were synthesized via [2+2] cycloaddition–retroelectrocyclization reaction of the ferrocenyl-substituted BODIPYs **8** and **9** in 83% and 85% yields, with TCNE at room temperature in dichloromethane.[58-63] We have reported the synthesis of meso-substituted BODIPY **7** and its TCBD derivative **10** (Scheme S2).[64-67] The control compounds meso, α, and β phenylacetylene substituted BODIPY **1–3** were synthesized by the palladium-catalyzed Sonogashira cross-coupling reaction of (meso-chloro), α-bromo, and β-iodo BODIPY with phenylacetylene (1 equiv.) in THF solvent at 60 °C in 80–90% yield.[68-69] Similarly meso, α, and β 1-ethynyl-4-(phenylacetylene) benzene substituted BODIPY **4–6** were synthesized by

Sonogashira cross-coupling reaction of meso-chloro, α-bromo, and β-iodo BODIPY with 1-ethynyl-4-(phenylacetylene) benzene (1 equiv) in THF solvent at 60 °C in 80–85% yield[68-69] (Scheme S2). The BODIPYs **7–9** and **10–12** were purified by repeated silica-gel column chromatography and recrystallization techniques.

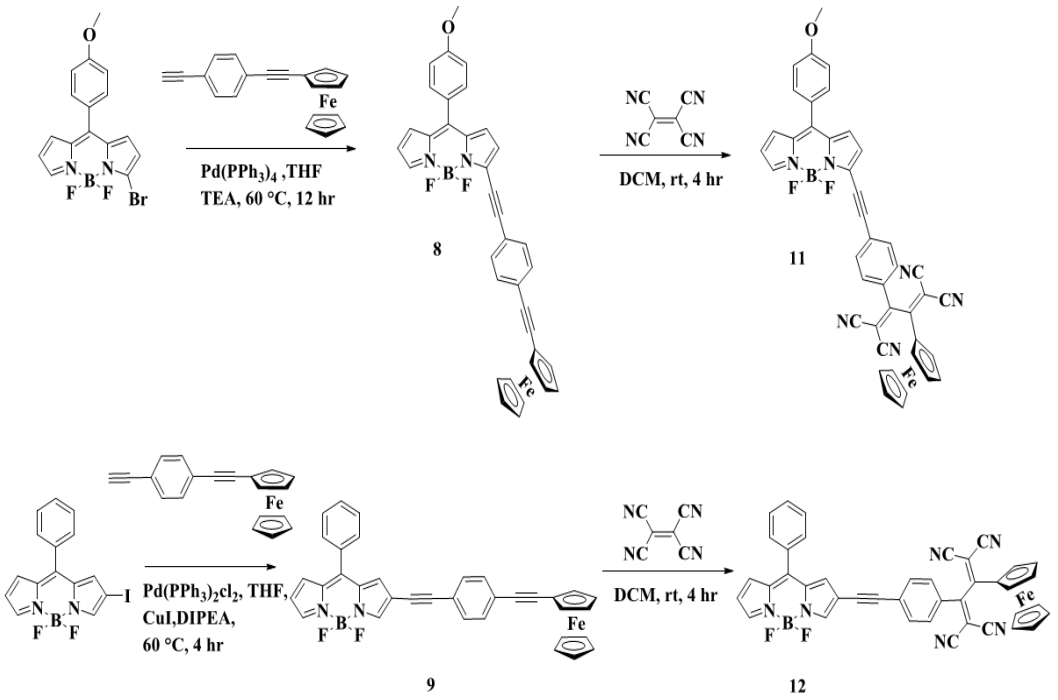

Scheme 1. Syntheses of differently substituted BODIPYs dyads 8–9 and triads 11–12.

The BODIPYs **7**–**9** and **10**–**12** exhibit good solubility in common organic solvents such as dichloromethane, toluene, chloroform, and benzonitrile and were well characterized by ^{1}H NMR, ^{13}C NMR, and HRMS techniques (See Figures S12-S35 in ESI for spectral details).

Absorbance and fluorescence studies

The electronic absorption and emission spectral studies of the differently substituted BODIPYs **1–6**, BODIPY-Fc dyads, **7–9**, and BODIPY-TCBD-Fc triads, **10–12** were performed in benzonitrile at room temperature as shown in Figures 3 and 4 while the data are summarized in Table 1. Pristine BODIPY is known to exhibit a strong absorption around 500 nm and fluorescence emission around 520 nm.[29-32] As shown in Figure 3, BODIPY with an acetylene group directly attached to the aryl π-system, a red-shifted absorption was observed. Interestingly, this red-shift was found to depend on the nature of substitution that followed the trend **2** > **3** > **1**. Having two acetylene linkers caused additional red-shift, and in this case the trend was **5** > **4** > **6** (Figure 3b).

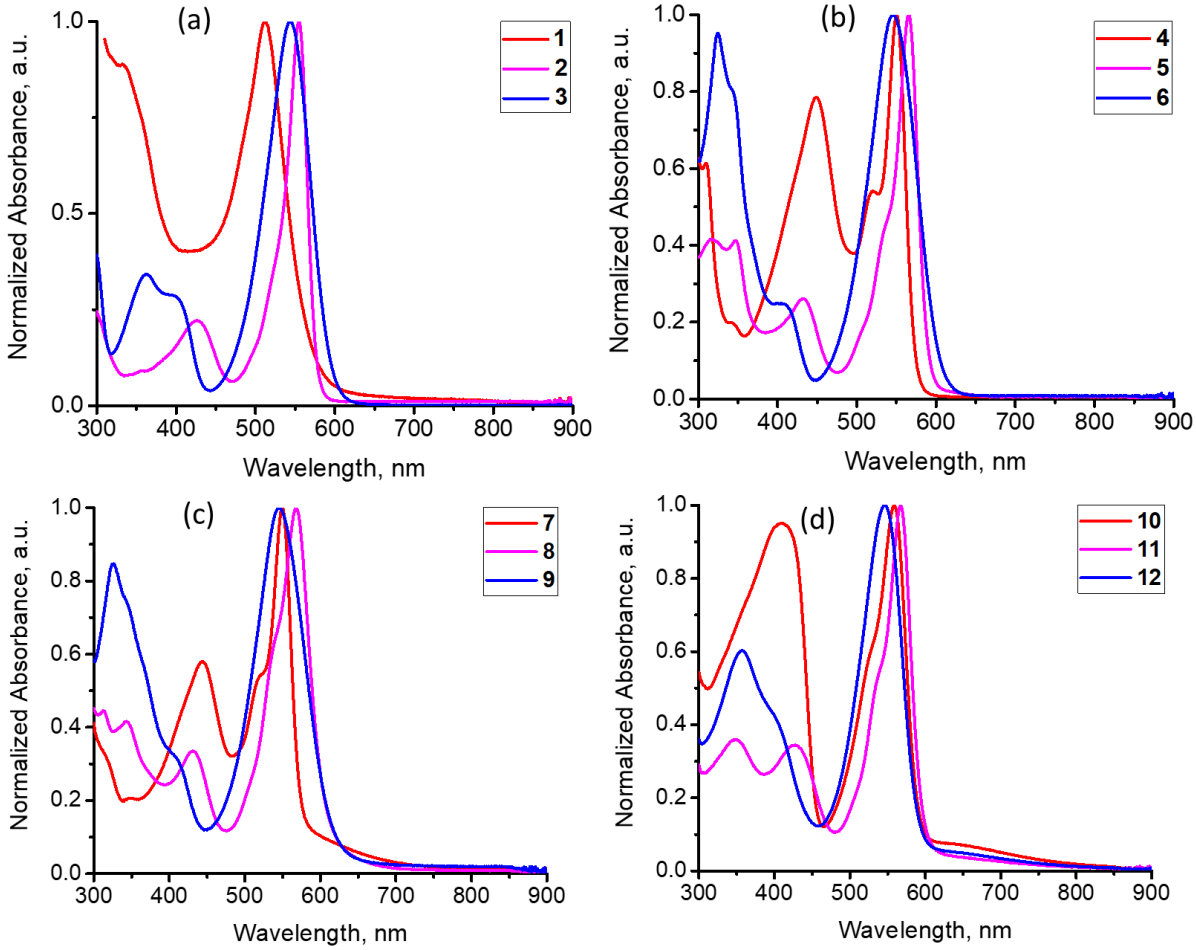

Figure 3. Normalized absorption spectra of the differently substituted BODIPYs **1**–**6** (a and b), BODIPY-Fc, **7**–**9** (c), and BODIPY-TCBD-Fc, **10**–**12** (d) in benzonitrile.

That is, highest red-shift was observed for α-pyrrole substituted derivatives. In the case of BODIPY-Fc systems, **7**–**9**, the observed trend was also similar (**8** > **7** > **9**), that is, higher red-shift was for dyad **8** having α-pyrrole functionalization, however, replacing the terminal phenyl ring with ferrocene in the dyads did not significantly change the peak position (Figure 3c). In the case of BODIPY-TCBD-Fc triads, **10**–**12**, having an electron withdrawing TCBD between the BODIPY and ferrocene entities, additional small red-shift of BODIPY with a trend in peak maxima following the order **11** > **10** > **12** (Figure 3d) was observed. These results illustrate substitution dependent absorption behavior of BODIPY probes in the dyads and triads. Another noteworthy observation was also made in the case of triads **10**–**12** where a weak, broad peak in the 600–800 nm range was observed. This has been attributed to the charge transfer interactions involving ferrocene and TCBD entities.[40-50]

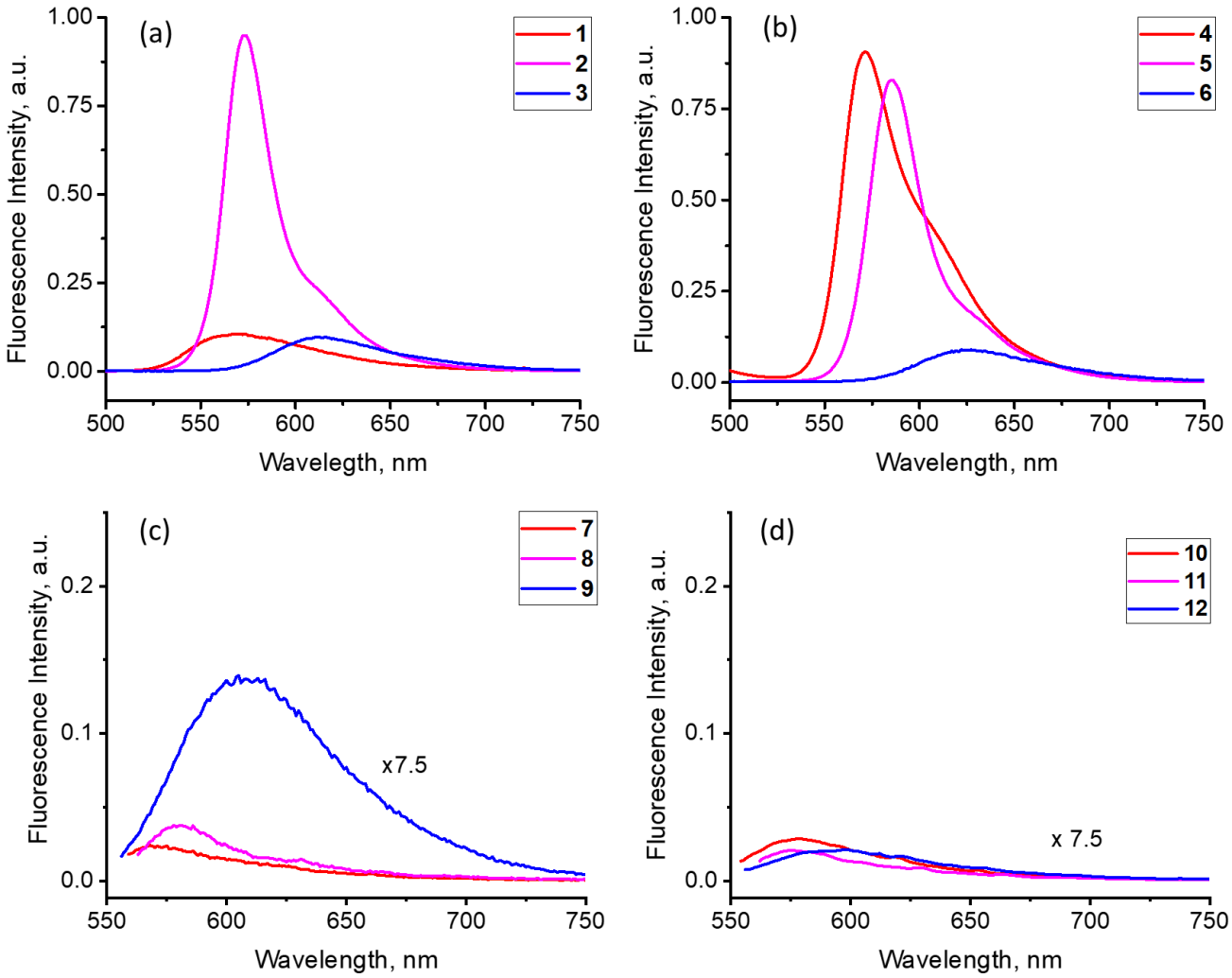

Figure 4. Normalized fluorescence spectra of differently substituted BODIPYs **1**–**6** (a and b), BODIPY-Fc, **7**–**9** (c), and BODIPY-TCBD-Fc, **10**–**12** (d) in benzonitrile. The samples were excited to the visible peak maxima given in Table 1.

Fluorescence spectra of the investigated compounds are shown in Figure 3 while the peak maxima and fluorescence lifetimes evaluated from time correlated single photon counting technique (TCSPC) are given in Table 1. For compounds **1**–**6** having either one or two acetylene π-extenders at different positions of the macrocycle periphery, appreciable fluorescence was observed. The following trends in fluorescence peak maxima were observed: **3** > **2** > **1** for the first three compounds and **6** > **5** > **4** for the last three compounds. For compounds **7**–**12** having either a terminal ferrocene or TCBD-Fc charge transfer entities, significant quenching of fluorescence was observed (95–98% compared to the corresponding control compound). The measured

fluorescence lifetimes for compounds **1**–**6** revealed lifetimes in the range of 1–6 ns. However, due to very low fluorescence emission no lifetime for compounds **7**–**12** could be obtained.

Table 1. Absorption and fluorescence peak maxima, fluorescence lifetime in ns, Stokes shift in cm^{-1}, and energy of the singlet excited state in eV of differently substituted BODIPYs 1–6, dyads 7–9, and triads 10–12 in benzonitrile (see Figure 1 for structures and Table S1 for data in toluene).

compound	λ_{abs} (nm)	λ_{em} (nm)	τ, ns	$\Delta\nu$ (cm^{-1})	$E_{0,0}$ (eV)
BODIPY	506	527	2.86	787	2.40
1	565	584	3.44	576	2.16
2	555	573	3.25	556	2.20
3	544	613	0.81	2069	2.14
4	550	569	6.06	607	2.22
5	546	625	0.59	2315	2.12
6	512	566	1.63	1863	2.30
7	550	568	--	576	2.22
8	568	580	--	364	2.16
9	545	608	--	1901	2.15
10	559	578	--	588	2.18
11	567	575	--	245	2.17
12	546	599	--	1621	2.17

The energy gap between the absorption and emission peak maxima (Stokes shift) was also estimated for the investigated series of compounds having substituents at different positions of the macrocycle periphery, as given in Table 1. For a given type of BODIPY derivative (monomers **1**–**6**, dyads **7**–**9**, or triads **10**–**12**), the highest energy gap was observed for β-pyrrole substituted derivatives (compounds **3, 6, 9**, and **12**) while the lowest gap was for α-pyrrole substituted derivatives (**2, 5, 8**, and **11**). Such shift for *meso*-substituted derivatives (**1, 4, 7**, and **10**) was intermediate between the β and α substituted BODIPY derivatives. A large Stokes shift helps in lowering inner filter effects and self-absorption in fluorescence.[70]

Singlet-singlet energy gap ($E_{0,0}$), also known as spectral HOMO-LUMO energy gap, was also evaluated from the absorption and emission data (mid-point energy), as listed in Table 1. For a given series of compounds, the highest gap was for *meso*-substituted derivatives (**1, 4, 7**, and **10**) while the lowest gap was for the *β*-pyrrole substituted derivatives (**3, 6, 9**, and **12**). Compared with pristine BODIPY, they were 0.10–0.35 eV lower as a consequence of the acetylene linker. The large Stokes shift observed for the latter series of compounds resulted in lowering the HOMO-LUMO gap. These findings bring out the importance of the effect of peripheral substitution in modulating the Stokes shifts and HOMO-LUMO gaps in BODIPY derivatives; a useful finding to develop the next generation of BODIPY based photo-probes.

Changing the solvent from polar benzonitrile to nonpolar toluene also revealed similar spectral trends. Spectral results in nonpolar toluene are shown in Figure S1 while the data are summarized in Table S1. In summary, position of BODIPY ring functionalization seem to retain spectral trends irrespective of polarity of the employed solvents.

Electrochemical and spectroelectrochemical studies

In order to probe the substitution effect on oxidation and reduction potentials of differently substituted BODIPYs (**1**–**6**) and those of BODIPY-Fc, **7**–**9** and BODIPY-TCBD-Fc, **10**–**12** systems, electrochemical studies using cyclic (CV) and differential pulse voltammetry (DPV) in benzonitrile containing 0.1 M (TBA)ClO_4 were performed. The reversibility of a given redox process was established from monitoring scan rate, and anodic to cathodic peak separation from cyclic voltammetric studies. Figure S2 shows the DPVs of the investigated compounds while the redox data according to the site of electron transfer are given in Table 2.

It may be mentioned here that the first BODIPY oxidation process was an irreversible process in almost all of these derivatives, hence DPV was used to secure the oxidation potentials. The BODIPY 2 has an electron-donating methoxy group, which lowered the first oxidation and increased the first reduction potentials which is reflective of the position of substituents (BODIPY **1 – 3**) and a difference in the electron-richness of BODIPY 2. Oxidation of Fc and reduction of TCBD were fully reversible on CV time scale in case of compounds **7 – 12**. Several interesting observations were made from the voltammograms and tabulated redox data (Table 2). For acetylene functionalized BODIPYs, **1**–**6**, facile oxidation (up to 0.37 V) compared to pristine BODIPY was observed. Such an effect on electrochemical reduction was marginal. This could be easily attributed to the extended π-conjugation of the acetylene linker in **1**–**6**. Introduction of a terminal

ferrocene entity in **7**–**9** revealed ferrocene oxidation that was anodically shifted by 0.11-0.14 V as compared to that of pristine ferrocene oxidation.[71] Perturbations in the BODIPY oxidation process in **7**–**9** was minimal. The presence of electron withdrawing TCBD group in compounds **10**–**12** revealed two one-electron reductions corresponding to the $TCBD^{0/\cdot-}$ and $TCBD^{\cdot-/2-}$ processes.[40-54] The first reduction process of TCBD was easier by 100–250 mV compared to the traditionally used fullerene electron acceptor.[8-9] The BODIPY reduction in these triads was more difficult to reduce and was cathodically shifted by ~100 mV. Due to close proximity of TCBD and ferrocene entities and the electronic interactions between them, the oxidation of ferrocene entity in the triads was harder by over 300 mV while for the oxidation of spatially far BODIPY entity this effect was marginal (~ 100 mV). In agreement with the earlier discussed optical results, electrochemical studies also revealed lower HOMO–LUMO gaps for the substituted BODIPY derivatives compared to pristine BODIPY.

The absorption spectral results shown in Figure 3 revealed peripheral substitution-dependent properties for the neutral BODIPY compounds. In an effort to visualize whether such an effect exists for one-electron oxidized and one-electron reduced products of the BODIPY derivatives, spectroelectrochemical studies were performed. Figure S3 for compounds **1**–**3** and Figure S4 for compounds **4**–**6** show differential absorption spectral changes observed during first oxidation and first reduction of the BODIPY derivatives. Subtle changes associated with one or more isosbestic points, including new peaks in few cases depending upon the site of substitution were observed.

Spectroelectrochemical studies on BODIPY-Fc, **7**–**9** and BODIPY-TCBD-Fc, **10**–**12** were also performed as such data would help in the interpretation of transient absorption data recorded to seek evidence of charge transfer/separation (*vide infra*). Spectral changes observed during first oxidation and first reduction of BODIPY-Fc systems is shown in Figure S5 while those of BODIPY-TCBD-Fc systems is given in Figure S6. The oxidation in both dyads and triads occur at the ferrocene entity, consequently, during this process spectral changes associated with BODIPY were minimal. In the case of dyads, the first reduction occurs at the BODIPY center, consequently, one could predict drastic spectral changes during this process. This is indeed the case as shown in Figure S5. A new peak at 720 nm for **7** was developed, however, no new peaks corresponding to $BODIPY^{\cdot-}$ in the case of **8** and **9** was observed. Interestingly, in the case of triads, where the first reduction involves TCBD, one would not expect much spectral changes for the BODIPY peaks, this entity is also associated with the reduction process. As shown in Figure S6, decrease in BODIPY Soret peak was witnessed in all three triads with new less intense peaks in

the visible region. These results indicate formation of $(BODIPY\text{-}TCBD)^{\cdot-}$ during the first reduction process, that is, delocalization of electron density on both BODIPY and TCBD entities. In both dyads and triads, the oxidation and reduction processes were accompanied by one or more isosbestic points.

Table 2. Electrochemical redox potentials (V. vs. Fc/Fc^{+}) of the investigated compounds in benzonitrile containing 0.1M $(TBA)ClO_4$.

compound	$BODIPY^{0/.-}$	$TCBD^{\cdot-/2-}$	$TCBD^{0/.+}$	$Fc^{0/+}$	$BODIPY^{0/.+}$
BODIPY	-1.17	--	--	--	1.19
1	-0.99	--	--	--	0.98
2	-1.13	--	--	--	0.86
3	-1.08	--	--	--	0.93
4	-0.89	--	--	--	1.06
5	-1.12	--	--	--	0.82
6	-1.09	--	--	--	0.99
7	-0.97	--	--	0.14	1.04
8	-1.16	--	--	0.13	0.97
9	-1.09	--	--	0.11	1.03
10		-1.11	-0.94	0.46	1.17
11	-1.21	-1.09	-0.75	0.46	1.08
12	-1.21	-1.07	-0.85	0.45	1.12

Further, the spectroelectrochemical data was used to deduce spectrum of the charge separated products. For this, spectrum of the cation and anion were digitally averaged and subtracted from that of the neutral compound.[45] Figure S7 shows such spectra of compounds **7 – 12**. Negative peaks indicate loss of intensity of the neutral compound while positive peaks represent absorption of either the radical cation or radical anion species. Such spectral data helps in analyzing transient spectral data that will be discussed later.

The density functional theory (DFT) calculations were performed to probe the substitution dependent delocalization of HOMOs and LUMOs as this could affect the ground and excited state interactions between the donor and acceptor entities of the investigated systems. Using the Gaussian 09 program, B3LYP/6-31+G** for C, H, O, N, B, F and Lanl2DZ for Fe level of theory and geometry optimization was carried out in the gas phase. The frontier molecular orbitals are displayed in Figure S8. The HOMO and LUMO of the ferrocenyl functionalized BODIPY **9** was localized on ferrocene and BODIPY entities, respectively. However, in the case of dyads **7** and **8**, although majority of the HOMO was on the expected ferrocene entity, part of the orbital coefficients was spread over the spacer into BODIPY. Majority of the LUMO was on BODIPY entity, as expected. In the case of triads **10-12**, LUMO was spread over TCBD and BODIPY entities, supporting earlier discussed $(BODIPY\text{-}TCBD)^{\cdot-}$ formation upon electroreduction.

Free-energy calculations and energy level diagram

Using the spectral and electrochemical data, Gibbs free-energy change associated for charge recombination and charge separation for different states were estimated according Rehm-Weller approach.[72] From the data presented in Table 3, it is clear that in the case of the BODIPY-Fc, **7**–**9** featuring BODIPY and ferrocene, formation of $BODIPY^{\bullet-}\text{-}Fc^{+}$ charge separated state from $^{1}BODIPY^{*}$ was a thermodynamically feasible process. Interestingly, in the case of BODIPY-

Table 3. Free-energy change for charge recombination (ΔG_{CR}) and charge separation (ΔG_{CS}) from the singlet excited state of BODIPY (=BDP in table) for the dyads and triads in benzonitrile.

Compound	$-\Delta G_{CR}$		$-\Delta G_{CS}$	
	$BDP^{\cdot-}/Fc^{+}$	$TCBD^{\cdot-}/Fc^{+}$	$BDP^{\cdot-}/Fc^{+}$	$TCBD^{\cdot-}/Fc^{+}$
7	1.15	--	1.07	--
8	1.33	--	0.83	--
9	1.24	--	0.91	--
10	1.72	1.56	0.48	0.62
11	1.71	1.37	0.45	0.80
12	1.71	1.46	0.46	0.71

TCBD-Fc, **10**–**12**, where TCBD$^{\delta+}$-Fc$^{\delta-}$ charge transfer in the ground state was witnessed, formation of initial (BODIPY-TCBD)$^{\delta-}$-Fc $^{\delta+}$ charge transfer complex from ^{1}BODIPY* is feasible. The (BODIPY-TCBD)$^{\delta-}$-Fc $^{\delta+}$ complex could subsequently generate energetically low-lying (BODIPY-TCBD)$^{-\bullet}$-Fc$^+$ charge separated state. Involvement of BODIPY in the final charge separation is confirmed by the earlier discussed spectroelectrochemical and computational studies.

Figure 5 shows an energy level diagram depicting the different photochemical events occurring in BODIPY-Fc systems (magenta colored arrows and energy states) and BODIPY-TCBD-Fc systems (blue colored arrows and energy states). In the case of BODIPY-Fc, reductive electron transfer from the ^{1}BODIPY* to yield the BODIPY$^{\bullet-}$-Fc$^+$ charge separated state is a

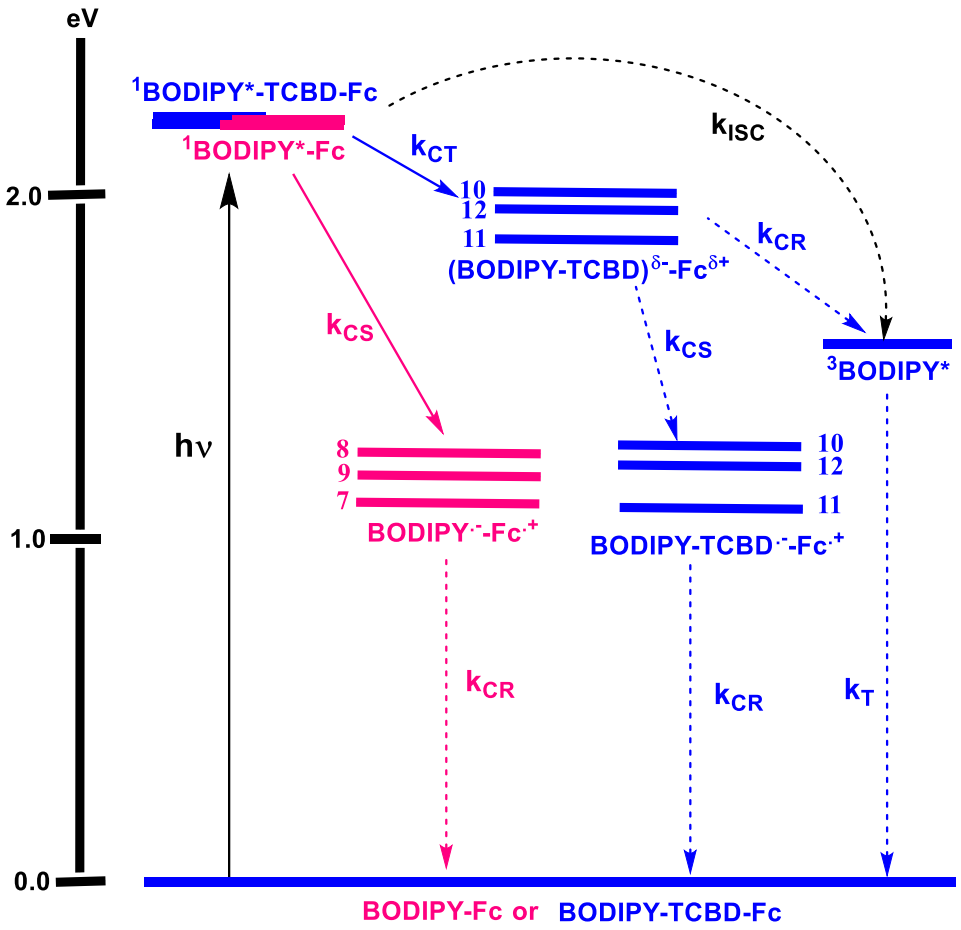

Figure 5. Energy level diagram showing the different photochemical events occurring in BODIPY-Fc, **7-9** (red), and BODIPY-TCBD-Fc (blue) **10-12** in benzonitrile. Energies of different states were evaluated from spectral and electrochemical studies. Solid arrows indicate major photo-processes, dashed arrow

indicates minor photo-processes. ISC = intersystem crossing, CT=charge transfer, CS = charge separation, CR = charge recombination, and T = emission from triplet excited state.

plausible deactivation path, and such a process is favored more in **7** compared to the other two dyads. Since the energy of the BODIPY$^{\bullet-}$-Fc^{+} charge separated state is lower than that of ^{3}BODIPY* (E_T = 1.48 eV),[73-76] direct charge recombination to the ground state could be envisioned. In the case of BODIPY-TCBD-Fc systems, formation of (BODIPY-TCBD)$^{\delta-}$-Fc $^{\delta+}$ charge transfer from the ^{1}BODIPY* is thermodynamically feasible. Since the energy of this state is higher than that of ^{3}BODIPY*,[73-76] population of the triplet level or charge separation to yield (BODIPY-TCBD)$^{-\bullet}$-Fc^{+} from the initial charge transfer states are possible. It is also important to note that due to high conducting acetylene linker and close proximity of the entities, faster photo-events could be envisioned. In order to verify such predictions, femtosecond transient spectral studies were performed and the results are presented in the following section.

Femtosecond transient absorption studies

Figure S9 show the fs-TA spectra at different delay times of BODIPY derivatives, **1 – 6** substituted with acetylene linkers at different peripheral positions. The instantaneously formed ^{1}BODIPY* revealed positive peaks in the 450 –550 nm range corresponding to transitions from the singlet excited state. In addition, a near-IR peak in the 900 –1400 nm range, (peak maxima depending upon the type of substitution, near-IR data not shown) corresponding to singlet-singlet transition from the ^{1}BODIPY* state were also observed. Negative peaks corresponding to ground state bleaching and stimulated emission were also observed whose peak minima correspond to peak maxima of the earlier discussed absorption and emission peaks of the respective BODIPY derivatives. The decay and recovery of the positive and negative peaks followed the lifetime of the individual compounds discussed earlier (see Table 1), sometime lasting longer than the monitoring time window of our instrumental setup of 3 ns. In summary, successful excitation of BODIPY to generate ^{1}BODIPY* irrespective of the position of peripheral acetylene substituents is accomplished.

Fs-TA spectra for selected BODIPY-Fc, and BODIPY-TCBD-Fc in benzonitrile are shown in Figure 6a-c while spectra coving the visible region for the investigated series are shown in Figure S10 in benzonitrile. As expected from the earlier discussed steady-state and time-resolved emission studies, relaxation of the ^{1}BODIPY* state was faster in both the cases of dyads and

triads, irrespective of the nature of peripheral substitution. The weak radical cation and radical anion signature peaks, viz., corresponding to BODIPY$^{\bullet-}$-Fc^{+} in the case of BODIPY-

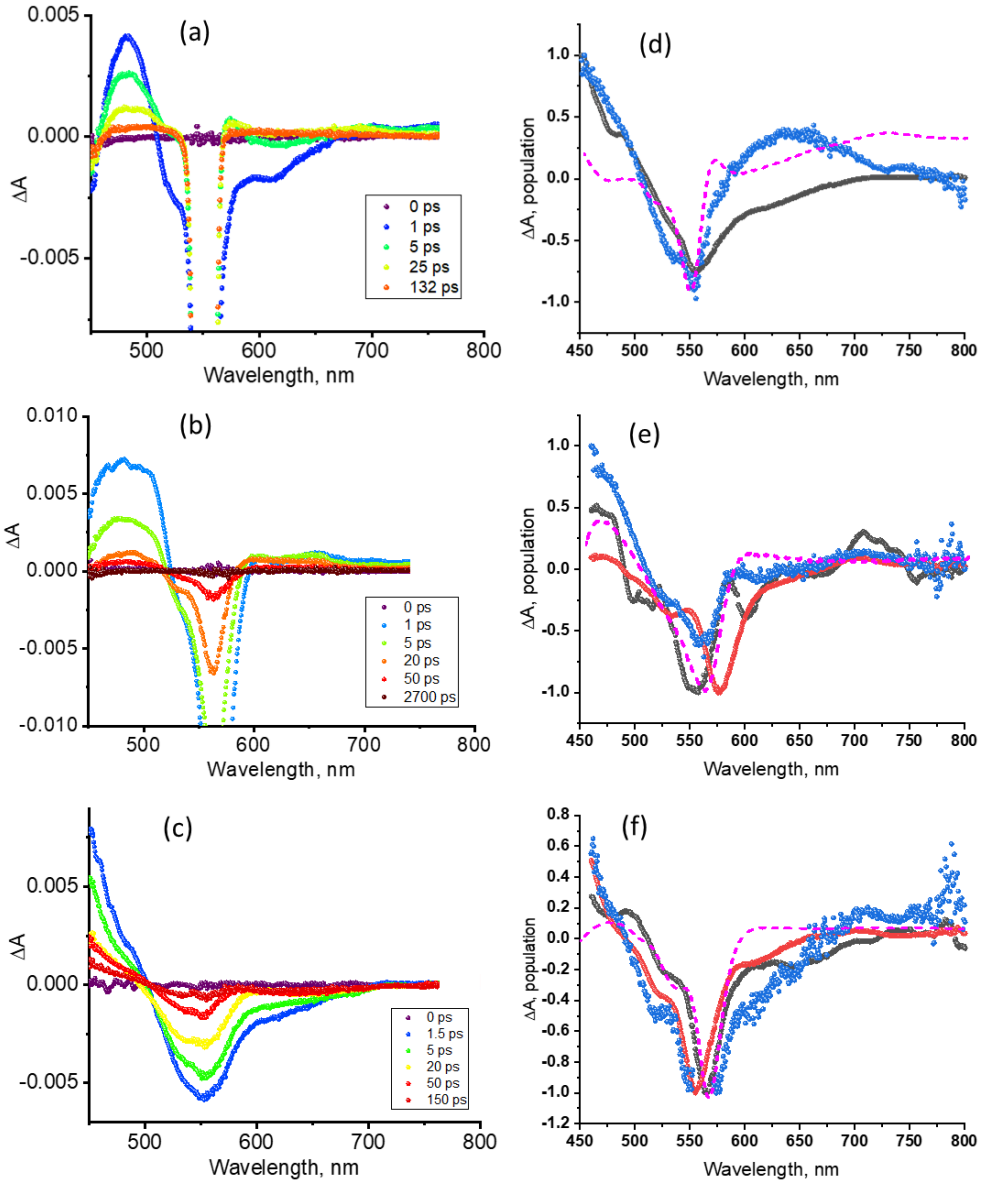

Figure 6. Femtosecond transient absorption spectra of (a) **7**, (b) **10**, and (c) **11** in Ar-saturated benzonitrile. The samples were excited at the visible peak maxima given in Table 1 (100 fs laser pulses) at room temperature. The species associated spectra (SAS) along with spectrum deduced from spectroelectrochemical studies for the charge separated state (dashed magenta line) for (d) **7**, (e) **10**, and (f) **11** are also shown.

Fc, and (BODIPY-TCBD)$^{\bullet-}$-Fc^{+} in the case of BODIPY-TCBD-Fc, were buried within the strong ^{1}BODIPY* induced signals.Target analysis[77,78] of the transient data was performed as shown in Figure 6d-f and Figure S11. A two component fit – representing formation of singlet excited state of BODIPY followed by charge separation in the case of BODIPY-Fc dyads, and a three

component fit in the case of triads, representing the formation of ^{1}BODIPY*, (BODIPY-TCBD)$^{\delta-}$-Fc$^{\delta+}$ charge transfer state, and (BODIPY-TCBD)$^{\bullet-}$-Fc$^+$ charge separated state gave satisfactory fitting. The spectrum generated for the charge separated species from spectroelectrochemical studies (Figure S7) largely matched that of the species associated spectra (SAS) corresponding to the charge separated products (see Figure 6 magenta line). This also helped in differentiating the SAS spectrum assigned for the charge transfer and charge separation states. Negative peaks in the SAS spectrum corresponding to charge transfer state were either 30-50 nm red-shifted (Figure 6e) or blue-shifted (Figure 6d), depending on the type of functionalization. However, peak minima of the spectrum corresponding to the charge separated state matched well with that spectrum deduced from spectroelectrochemical studies, thus supporting the charge transfer → charge separation process in these triads.

Table 4. Time constants (in ps) for charge separation and recombination for the dyads 7–9 and triads 10–12 in benzonitrile (estimated error = ±10%).

Compound	τ_S/τ_{CT},[a,b] ps	τ_{CS}, ps
7	1.410	114.0
8	0.330	537.0
9	0.030	270.1
10	0.690	15.2
11	1.170	17.6
12	1.170	25.5

[a]τ_S corresponds to the formation of ^{1}BODIPY* in the case of dyads. [b]τ_{CT} corresponds to the formation of (BODIPY-TCBD)$^{\delta-}$-Fc $^{\delta+}$ charge transfer state in the case of triads

Time constants from population time profiles for different photo-events are given in Table 4. In the case of triads, formation of S_1 state was within the time resolution of our instrumental setup (< 500 fs), so only time constants of charge transfer and charge separation states are listed. The magnitude of time constants revealed occurrence of ultrafast charge separation more so in the case of triads having a stronger electron acceptor, TCBD. With respect to the location of functionalization of dyads, time constants for the BODIPY$^{\bullet-}$-Fc$^+$ charge separated state followed the order **8** > **9** > **7**. That is, the charge separated state lasted longer in pyrrole ring functionalized

BODIPY derivatives compered to that of meso-functionalized ones. A comparison of these results with the energy of charge separated states in Figure 4 suggests that this process to belong to the inverted Marcus region.[79] That is, charge stabilization (slow charge recombination process) with increase in free-energy is observed. In the case of triads producing (BODIPY-TCBD)$^{\bullet-}$-Fc^{+} charge separated states, the time constants of the charge separated states were short and very close (15-25 ps) due to high exothermicity associated with the charge recombination process, nonetheless the following order was observed: **12** > **11** > **10**. That is, performance of pyrrole ring functionalized derivatives in terms of charge stabilization was better.

CONCLUSIONS

In summary, structure-property correlations with respect to the location of peripheral functionalization of BODIPY on its optical absorbance, fluorescence, and electrochemical studies have been accomplished. Among the *meso*-, α- or β-pyrrole derivatized BODIPYs, $E_{0,0}$ and Stokes shift were found to depend upon the nature of substitution. The Stokes shift followed the order β- > *meso* > α- substitution for a given series of BODIPY derivatives while the $E_{0,0}$ followed the order *meso* > α- > β- substitution. The performed electrochemical studies helped in the determination of redox potentials of the different entities of dyads and triads. Formation of BODIPY$^{\bullet-}$-Fc^{+} charge separated state in the case of dyads, and (BODIPY-TCBD)$^{\bullet-}$-Fc^{+} charge separated states in the case of triads was possible to envision from the free-energy calculations, and by the established energy level diagram. Consequently, significant quenching of BODIPY fluorescence (> 95%, both steady-state and time-resolved) in both dyads and triads irrespective of the nature of peripheral substitution was observed. Fs-TA studies coupled with target analysis of spectral data revealed occurrence of ultrafast charge separation from the ^{1}BODIPY* in these donor-acceptor systems. The measured time constants point to an important conclusion that the pyrrole ring functionalized derivatives revealed better charge stabilization over the meso-functionalized ones. Collectively, the reported spectral and photochemical results are important in designing a new generation of fluorescence probes and sensors, as well as in artificial photosynthesis involving light energy harvesting.

ASSOCIATED CONTENT

Supporting Information.

Experimental section, Additional spectral, spectroelectrochemical, and femtosecond spectra, ^{1}H and ^{13}C NMR and HRMS of triads. This material is available free of charge via the Internet at http://pubs.acs.org."

AUTHOR INFORMATION

Corresponding Authors

Rajneesh Misra - Department of Chemistry, Indian Institute of Technology, Indore 453552, India. E-mail: rajneeshmisra@iiti.ac.in;

Francis D'Souza - Department of Chemistry, University of North Texas, 1155 Union Circle, #305070, 76203-5017, Denton, TX, USA.E-mail: Francis.DSouza@UNT.edu; ORCID: 0000-0003-3815-8949

Authors

Jivan S. Shinde - Department of Chemistry, Indian Institute of Technology, Indore 453552, India.

Michael B. Thomas - Department of Chemistry, University of North Texas, 1155 Union Circle, #305070, 76203-5017, Denton, TX, USA.

Madhurima Poddar - Department of Chemistry, Indian Institute of Technology, Indore 453552, India

Author Contributions

‡ These authors contributed equally.

ACKNOWLEDGMENT

Support by the US-National Science Foundation (grant no. 2000988 to FD) is acknowledged. RM acknowledges the support by SERB Project No. (Project No. CRG/2018/000032), and Council of Scientific and Industrial Research (Project No. 01(2934)/18/EMR-II), New Delhi. We also thank the Sophisticated Instrumentation Centre (SIC), Indian Institute of Technology (IIT) Indore.

REFERENCES

(1) Deisenhofer, J.; Epp, O.; Miki, K.; Huber R.; Michel, H. X-ray Structure Analysis of a Membrane Protein Complex. *J. Mol. Biol.*, 1984, 180, 385.

(2) *Handbook of Photosynthesis*, 2nd ed. (Ed.: M. Pessarakli), CRC, Boca Raton, **2005**.

(3) Wasielewski, M. R. Self-Assembly Strategies for Integrating Light Harvesting and Charge Separation in Artificial Photosynthetic Systems. *Acc. Chem. Res.* **2009**, *42* (12), 1910–1921.

(4) Gust, D.; Moore, T. A.; Moore, A. L. Solar Fuels via Artificial Photosynthesis. *Acc. Chem. Res.* **2009**, *42* (12), 1890–1898.

(5) Armaroli, N.; Balzani, V. Die Zukunft der Energieversorgung – Herausforderungen und Chancen. *Angew. Chem.* **2007**, *119* (1–2), 52–67, The Future of Energy Supply: Challenges and Opportunities. *Angew. Chem. Int. Ed.* **2007**, *46* (1–2), 52–66.

(6) Sánchez, L.; Martín, N.; Guldi, D. M. Wasserstoffbrückenmotive in der Fullerenchemie. *Angew. Chem.* **2005**, *117* (34), 5508–5516, Hydrogen-Bonding Motifs in Fullerene Chemistry. *Angew. Chem. Int. Ed.* **2005**, *44* (34), 5374–5382.

(7) Sgobba, V.; Guldi, D. M. Carbon Nanotubes—Electronic/Electrochemical Properties and Application for Nanoelectronics and Photonics. *Chem Soc Rev* **2009**, *38* (1), 165–184.

(8) Imahori, H.; Fukuzumi, S. Porphyrin and Fullerene based molecular photovoltaic devices. *Adv. Funct. Mater.* **2004**, 14, 525.

(9) Fukuzumi, S. Development of Bioinspired Artificial Photosynthetic Systems. *Phys. Chem. Chem. Phys.* **2008**, *10* (17), 2283.

(10) Torres, T.; Bottari, G. Organic Nanomaterials Eds. Wiley-VCH, Weinheim. **2013**, 187-204.

(11) Ito, O.; D'Souza, F. Functionalized Nanocarbons for Artificial Photosynthesis: From Fullerene to SWCNT, Carbon Nanohorn, and Graphene. In *From Molecules to Materials*; Rozhkova, E. A., Ariga, K., Eds.; Springer International Publishing: Cham, 2015; pp 193–240.

(12) Sessler, J. L.; Lawrence, C. M.; Jayawickramarajah, J. Molecular Recognition via Base-Pairing. *Chem Soc Rev* **2007**, *36* (2), 314–325.

(13) Claessens, C. G.; González-Rodríguez, D.; Rodríguez-Morgade, M. S.; Medina, A.; Torres, T. Subphthalocyanines, Subporphyrazines, and Subporphyrins: Singular Nonplanar Aromatic Systems. *Chem. Rev.* **2014**, *114* (4), 2192–2277.

(14) Bottari, G.; de la Torre, G.; Guldi, D. M.; Torres, T. Covalent and Noncovalent Phthalocyanine−Carbon Nanostructure Systems: Synthesis, Photoinduced Electron Transfer, and Application to Molecular Photovoltaics. *Chem. Rev.* **2010**, *110* (11), 6768–6816.

(15) D'Souza, F.; Ito, O. Photosensitized Electron Transfer Processes of Nanocarbons Applicable to Solar Cells. *Chem Soc Rev* **2012**, *41* (1), 86–96.

(16) Wang, J.-L.; Xiao, Q.; Pei, J. Benzothiadiazole-Based D−π-A−π-D Organic Dyes with Tunable Band Gap: Synthesis and Photophysical Properties. *Org. Lett.* **2010**, *12* (18), 4164–4167.

(17) Bureš, F.; Schweizer, W. B.; May, J. C.; Boudon, C.; Gisselbrecht, J.-P.; Gross, M.; Biaggio, I.; Diederich, F. Property Tuning in Charge-Transfer Chromophores by Systematic Modulation of the Spacer between Donor and Acceptor. *Chem. - Eur. J.* **2007**, *13* (19), 5378–5387.

(18) Liu, J.-Y.; Yeung, H.-S.; Xu, W.; Li, X.; Ng, D. K. P. Highly Efficient Energy Transfer in Subphthalocyanine−BODIPY Conjugates. *Org. Lett.* **2008**, *10* (23), 5421–5424.

(19) Maligaspe, E.; Kumpulainen, T.; Subbaiyan, N. K.; Zandler, M. E.; Lemmetyinen, H.; Tkachenko, N. V.; D'Souza, F. Electronic energy harvesting multi BODIPY-zinc porphyrin dyads accommodating fullerene as photosynthetic composite of antenna-reaction center. *Phys. Chem. Chem. Phys.* **2010**, 12, 7434-7444.

(20) Ziessel, R.; Retailleau, P.; Elliott, K. J.; Harriman, A. Boron Dipyrrin Dyes Exhibiting "Push–Pull–Pull" Electronic Signatures. *Chem. Eur. J.* **2009**, 15, 10369-10374.

(21) Rousseau, T.; Cravino, A.; Ripaud, E.; Leriche, P.; Rihn, S.; De Nicola, A.; Ziessel, R.; Roncali, J. A Tailored Hybrid BODIPY–Oligothiophene Donor for Molecular Bulk Heterojunction Solar Cells with Improved Performances. *Chem. Commun.* **2010**, *46* (28), 5082.

(22) Shao, S.; Gobeze, H. B.; Karr, P. A.; D'Souza, F. Ultrafast Photoinduced Charge Separation in Wide-Band-Capturing Self-Assembled Supramolecular Bis(Donor Styryl)BODIPY-Fullerene Conjugates. *Chem. - Eur. J.* **2015**, *21* (45), 16005–16016.

(23) Badgurjar, D.; Seetharaman, S.; D'Souza, F.; Chitta, R. One-Photon Excitation Followed by a Three-Step Sequential Energy–Energy–Electron Transfer Leading to a Charge-Separated State in a Supramolecular Tetrad Featuring Benzothiazole–Boron-Dipyrromethene–Zinc Porphyrin–C_{60}. *Chem. – Eur. J.* **2021**, *27* (6), 2184–2195.

(24) Chahal, M. K.; Liyanage, A.; Gobeze, H. B.; Payne, D. T.; Ariga, K.; Hill, J. P.; D'Souza, F. Supramolecular Ultrafast Energy and Electron Transfer in a Directly Linked BODIPY–Oxoporphyrinogen Dyad upon Fluoride Ion Binding. *Chem. Commun.* **2020**, *56* (27), 3855–3858.

(25) Zarrabi, N.; Obondi, C. O.; Lim, G. N.; Seetharaman, S.; Boe, B. G.; D'Souza, F.; Poddutoori, P. K. Charge-Separation in Panchromatic, Vertically Positioned Bis(Donor Styryl)BODIPY–Aluminum(III) Porphyrin–Fullerene Supramolecular Triads. *Nanoscale* **2018**, *10* (44), 20723–20739.

(26) Cantu, R.; Seetharaman, S.; Babin, E. M.; Karr, P. A.; D'Souza, F. Paddle-Wheel BODIPY–Hexaoxatriphenylene Conjugates: Participation of Redox-Active Hexaoxatriphenylene in Excited-State Charge Separation to Yield High-Energy Charge-Separated States. *J. Phys. Chem. A* **2018**, *122* (15), 3780–3786.

(27) Lewis, N. S.; Nocera, D. G. Powering the Planet: Chemical Challenges in Solar Energy Utilization. *Proc. Natl. Acad. Sci.* **2006**, *103* (43), 15729–15735.

(28) Kamat, P. V. Meeting the Clean Energy Demand: Nanostructure Architectures for Solar Energy Conversion. *J. Phys. Chem. C* **2007**, *111* (7), 2834–2860.

(29) Loudet, A.; Burgess, K. BODIPY Dyes and Their Derivatives: Syntheses and Spectroscopic Properties. *Chem. Rev.* **2007**, *107* (11), 4891–4932.

(30) Boens, N.; Leen, V.; Dehaen, W. Fluorescent Indicators Based on BODIPY. *Chem Soc Rev* **2012**, *41* (3), 1130–1172.

(31) Kowada, T.; Maeda, H.; Kikuchi, K. BODIPY-Based Probes for the Fluorescence Imaging of Biomolecules in Living Cells. *Chem. Soc. Rev.* **2015**, *44* (14), 4953–4972.

(32) El-Khouly, M. E.; Fukuzumi, S.; D'Souza, F. Photosynthetic Antenna-Reaction Center Mimicry by Using Boron Dipyrromethene Sensitizers. *ChemPhysChem* **2014**, *15* (1), 30–47.

(33) Ulrich, G.; Ziessel, R.; Harriman, A. The Chemistry of Fluorescent Bodipy Dyes: Versatility Unsurpassed. *Angew. Chem. Int. Ed.* **2008**, *47* (7), 1184–1201.

(34) Engelhardt, V.; Kuhri, S.; Fleischhauer, J.; García-Iglesias, M.; González-Rodríguez, D.; Bottari, G.; Torres, T.; Guldi, D. M.; Faust, R. Light-Harvesting with Panchromatically Absorbing BODIPY–Porphyrazine Conjugates to Power Electron Transfer in Supramolecular Donor–Acceptor Ensembles. *Chem. Sci.* **2013**, *4* (10), 3888.

(35) Zatsikha, Y. V.; Maligaspe, E.; Purchel, A. A.; Didukh, N. O.; Wang, Y.; Kovtun, Y. P.; Blank, D. A.; Nemykin, V. N. Tuning Electronic Structure, Redox, and Photophysical Properties in Asymmetric NIR-Absorbing Organometallic BODIPYs. *Inorg. Chem.* **2015**, *54*, 7915−7928.

(36) Qin, W.; Rohand, T.; Dehaen, W.; Clifford, J. N.; Driesen, K.; Beljonne, D.; Averbeke, B. V. Boron Dipyrromethene Analogs with Phenyl, Styryl, and Ethynylphenyl Substituents: Synthesis, Photophysics, Electrochemistry, and Quantum-Chemical Calculations. 10.

(37) Bandi, V.; Das, S. K.; Awuah, S. G.; You, Y.; D'Souza, F. Thieno-Pyrrole-Fused 4,4-Difluoro-4-Bora-3a,4a-Diaza- *s* -Indacene–Fullerene Dyads: Utilization of Near-Infrared Sensitizers for Ultrafast Charge Separation in Donor–Acceptor Systems. *J. Am. Chem. Soc.* **2014**, *136*, 7571–7574.

(38) Shao, S.; Thomas, M. B.; Park, K. H.; Mahaffey, Z.; Kim, D.; D'Souza, F. Sequential Energy Transfer Followed by Electron Transfer in a BODIPY–BisstyrylBODIPY Bound to C_{60} Triad *via* a 'Two-Point' Binding Strategy. *Chem. Commun.* **2018**, *54*, 54–57.

(39) Kivala, M.; Boudon, C.; Gisselbrecht, J.-P.; Seiler, P.; Gross, M.; Diederich, F. Charge-Transfer Chromophores by Cycloaddition-Retro-Electrocyclization: Multivalent Systems and Cascade Reactions. *Angew. Chem. Int. Ed.* **2007**, *46*, 6357–6360.

(40) Sekita, M.; Ballesteros, B.; Diederich, F.; Guldi, D. M.; Bottari, G.; Torres, T. Intense Ground-State Charge-Transfer Interactions in Low-Bandgap, Panchromatic Phthalocyanine–Tetracyanobuta-1,3-diene Conjugates. *Angew. Chem. Int. Ed.* **2016**, *55*, 5560–5564.

(41) Winterfeld, K. A.; Lavarda, G.; Guilleme, J.; Sekita, M.; Guldi, D. M.; Torres, T.; Bottari, G. Subphthalocyanines Axially Substituted with a Tetracyanobuta-1,3-Diene–Aniline Moiety: Synthesis, Structure, and Physicochemical Properties. *J. Am. Chem. Soc.* **2017**, *139*, 5520–5529.

(42) Winterfeld, K. A.; Lavarda, G.; Guilleme, J.; Guldi, D. M.; Torres, T.; Bottari, G. Subphthalocyanine–Tetracyanobuta-1,3-Diene–Aniline Conjugates: Stereoisomerism and Photophysical Properties. *Chem. Sci.* **2019**, *10*, 10997–11005.

(43) Gotfredsen, H.; Neumann, T.; Storm, F. E.; Muñoz, A. V.; Jevric, M.; Hammerich, O.; Mikkelsen, K. V.; Freitag, M.; Boschloo, G.; Nielsen, M. B. Donor−Acceptor-Functionalized Subphthalocyanines for Dye-Sensitized Solar Cells. *ChemPhotoChem* **2018**, *2*, 976–985.

(44) Gautam, P.; Misra, R.; Thomas, M. B.; D'Souza, F. Ultrafast Charge-Separation in Triphenylamine-BODIPY-Derived Triads Carrying Centrally Positioned, Highly Electron-Deficient, Dicyanoquinodimethane or Tetracyanobutadiene Electron-Acceptors. *Chem. – Eur. J.* **2017**, *23*, 9192–9200.

(45) Sharma, R.; Thomas, M. B.; Misra, R.; D'Souza, F. Strong Ground- and Excited-State Charge Transfer in C_3-Symmetric Truxene-Derived Phenothiazine-Tetracyanobutadine and Expanded Conjugates. *Angew. Chem. Int. Ed.* **2019**, *58*, 4350–4355.

(46) Rout, Y.; Jang, Y.; Gobeze, H. B.; Misra, R.; D'Souza, F. Conversion of Large-Bandgap Triphenylamine–Benzothiadiazole to Low-Bandgap, Wide-Band Capturing Donor–Acceptor Systems by Tetracyanobutadiene and/or Dicyanoquinodimethane Insertion for Ultrafast Charge Separation. *J. Phys. Chem. C* **2019**, *123*, 23382–23389.

(47) Poddar, M.; Jang, Y.; Misra, R.; D'Souza, F. Excited-State Electron Transfer in 1,1,4,4-Tetracyanobuta-1,3-diene (TCBD)- and Cyclohexa-2,5-diene-1,4-diylidene-Expanded TCBD-Substituted BODIPY-Phenothiazine Donor–Acceptor Conjugates. *Chem. – Eur. J.* **2020**, *26*, 6869–6878.

(48) Pinjari, D.; Alsaleh, A. Z.; Patil, Y.; Misra, R.; D'Souza, F. Interfacing High-Energy Charge-Transfer States to a Near-IR Sensitizer for Efficient Electron Transfer upon Near-IR Irradiation. *Angew. Chem. Int. Ed.* **2020**, *59*, 23697–23705.

(49) Yadav, I. S.; Alsaleh, A. Z.; Misra, R.; D'Souza, F. Charge Stabilization *via* Electron Exchange: Excited Charge Separation in Symmetric, Central Triphenylamine Derived, Dimethylaminophenyl–Tetracyanobutadiene Donor–Acceptor Conjugates. *Chem. Sci.* **2021**, *12*, 1109–1120.

(50) Jang, Y.; Rout, Y.; Misra, R.; D'Souza, F. Symmetric and Asymmetric Push–Pull Conjugates: Significance of Pull Group Strength on Charge Transfer and Separation. *J. Phys. Chem. B* **2021**, *125*, 4067–4075.

(51) Michinobu, T.; Boudon, C.; Gisselbrecht, J.-P.; Seiler, P.; Frank, B.; Moonen, N. N. P.; Gross, M.; Diederich, F. Donor-Substituted 1,1,4,4-Tetracyanobutadienes (TCBDs): New Chromophores with Efficient Intramolecular Charge-Transfer Interactions by Atom-Economic Synthesis. *Chem. - Eur. J.* **2006**, *12*, 1889–1905.

(52) Tancini, F.; Monti, F.; Howes, K.; Belbakra, A.; Listorti, A.; Schweizer, W. B.; Reutenauer, P.; Alonso-Gómez, J.-L.; Chiorboli, C.; Urner, L. M.; Gisselbrecht, J.-P.; Boudon, C.; Armaroli, N.; Diederich, F. Cyanobuta-1,3-Dienes as Novel Electron Acceptors for Photoactive Multicomponent Systems. *Chem. - Eur. J.* **2014**, *20*, 202–216.

(53) Koszelewski, D.; Nowak-Król, A.; Gryko, D. T. Selective Cycloaddition of Tetracyanoethene (TCNE) and 7,7,8,8-Tetracyano- *p* -quinodimethane (TCNQ) to Afford *Meso* -Substituted Phenylethynyl Porphyrins. *Chem. – Asian J.* **2012**, *7*, 1887–1894.

(54) Wu, Y.-L.; Stuparu, M. C.; Boudon, C.; Gisselbrecht, J.-P.; Schweizer, W. B.; Baldridge, K. K.; Siegel, J. S.; Diederich, F. Structural, Optical, and Electrochemical Properties of Three-Dimensional Push–Pull Corannulenes. *J. Org. Chem.* **2012**, *77*, 11014–11026.

(55) Paek, S.; Cho, N.; Cho, S.; Lee, J. K.; Ko, J. Planar Star-Shaped Organic Semiconductor with Fused Triphenylamine Core for Solution-Processed Small-Molecule Organic Solar Cells and Field-Effect Transistors. *Org. Lett.* **2012**, *14*, 6326–6329.

(56) Yuan, W. Z.; Gong, Y.; Chen, S.; Shen, X. Y.; Lam, J. W. Y.; Lu, P.; Lu, Y.; Wang, Z.; Hu, R.; Xie, N.; Kwok, H. S.; Zhang, Y.; Sun, J. Z.; Tang, B. Z. Efficient Solid Emitters with Aggregation-Induced Emission and Intramolecular Charge Transfer Characteristics: Molecular Design, Synthesis, Photophysical Behaviors, and OLED Application. *Chem. Mater.* **2012**, *24*, 1518–1528.

(57) Wijesinghe, C. A.; El-Khouly, M. E.; Zandler, M. E.; Fukuzumi, S.; D'Souza, F. A Charge-Stabilizing, Multimodular, Ferrocene-Bis(Triphenylamine)-Zinc-Porphyrin-Fullerene Polyad. *Chem. - Eur. J.* **2013**, *19*, 9629–9638.

(58) Rohand, T.; Baruah, M.; Qin, W.; Boens, N.; Dehaen, W. Functionalisation of Fluorescent BODIPY Dyes by Nucleophilic Substitution. *Chem Commun* **2006**, No. 3, 266–268.

(59) Lakshmi, V.; Ravikanth, M. Brominated Boron Dipyrrins: Synthesis, Structure, Spectral and Electrochemical Properties. *Dalton Trans.* **2012**, *41*, 5903-5911.

(60) Khan, T. K.; Ravikanth, M. Synthesis of Covalently Linked Boron–Dipyrromethene–Chromophore Conjugates Using 3-Bromo Boron–Dipyrromethene as a Key Precursor. *Tetrahedron* **2011**, *67*, 5816–5824.

(61) Rao, M. R.; Kumar, K. V. P.; Ravikanth, M. Synthesis of Boron-Dipyrromethene–Ferrocene Conjugates. *J. Organomet. Chem.* **2010**, *695*, 863–869.

(62) Ziessel, R.; Retailleau, P.; Elliott, K. J.; Harriman, A. Boron Dipyrrin Dyes Exhibiting "Push-Pull-Pull" Electronic Signatures. *Chem. - Eur. J.* **2009**, *15*, 10369–10374.

(63) Nemykin, V. N.; Purchel, A. A.; Spaeth, A. D.; Barybin, M. V. Probing the Electronic Properties of a Trinuclear Molecular Wire Involving Isocyanoferrocene and Iron(II) Phthalocyanine Motifs. *Inorg. Chem.* **2013**, *52*, 11004–11012.

(64) Dhokale, B.; Gautam, P.; Mobin, S. M.; Misra, R. Donor–Acceptor, Ferrocenyl Substituted BODIPYs with Marvelous Supramolecular Interactions. *Dalton Trans* **2013**, *42*, 1512–1518.

(65) An, D.-L.; Zhang, Z.; Orita, A.; Mineyama H.; Otera, J. Convenient Synthesis of (1-Propynyl)arenes through a One-Pot Double Elimination Reaction, and Their Conversion to Enynes. *Synlett.* **2007**, No. 12, 1909–1912.

(66) Ma, J.; Krauße, N.; Butenschön, H. 1,1′-Dialkynylferrocenes as Substrates for Bidirectional Alkyne Metathesis Reaction: 1,1′-Dialkynylferrocenes in Bidirectional Alkyne Metathesis Reactions. *Eur. J. Org. Chem.* **2015**, *2015*, 4510–4518.

(67) Krauße, N.; Kielmann, M.; Ma, J.; Butenschön, H. Reactions of Alkynyl- and 1,1′-Dialkynylferrocenes with Tetracyanoethylene - Unanticipated Addition at the *Less* Electron-Rich of Two Triple Bonds: Reactions of Alkynylferrocenes with Tetracyanoethylene. *Eur. J. Org. Chem.* **2015**, *2015*, 2622–2631.

(68) Dhokale, B.; Jadhav, T.; Mobin, S. M.; Misra, R. Tetracyanobutadiene Functionalized Ferrocenyl BODIPY Dyes. *Dalton Trans.* **2016**, *45*, 1476–1483.

(69) Patil, Y.; Misra, R.; Keshtov, M. L.; Sharma, G. D. 1,1,4,4-Tetracyanobuta-1,3-Diene Substituted Diketopyrrolopyrroles: An Acceptor for Solution Processable Organic Bulk Heterojunction Solar Cells. *J. Phys. Chem. C* **2016**, *120*, 6324–6335.

(70) Lakowicz, J. R. Principles of Fluorescence Spectroscopy, 3rd ed., Springer: Singapore, **2006**.

(71) Misra, R.; Jadhav, T.; Nevonen, D.; Mono, E. M.; Mobin, S. M.; Nemykin, V. N. Syntheis, Structures, and Redox Properties of Tetracyano-Bridged Diferrocene Donor-Acceptor Systems, *Organometallics*, **2017**, *36*, 4490-4498.

(72) Rehm, D.; Weller, A. Kinetics of Fluorescence Quenching by Electron and H-Atom Transfer. *Isr. J. Chem.* **1970**, *8*, 259–271.

(73) Bandi, V.; Gobeze, H. B.; Lakshmi, V.; Ravikanth, M.; D'Souza, F. Vectorial Charge Separation and Selective Triplet-State Formation during Charge Recombination in a Pyrrolyl-Bridged BODIPY–Fullerene Dyad. *J. Phys. Chem. C* **2015**, *119*, 8095–8102.

(74) Sharma, R.; Gobeze, H. B.; D'Souza, F.; Ravikanth, M. Panchromatic Light Capture and Efficient Excitation Transfer Leading to Near-IR Emission of BODIPY Oligomers. *ChemPhysChem* **2016**, *17*, 2516–2524.

(75) Shao, S.; Gobeze, H. B.; Bandi, V.; Funk, C.; Heine, B.; Duffy, M. J.; Nesterov, V.; Karr, P. A.; D'Souza, F. Triplet BODIPY and AzaBODIPY Derived Donor-acceptor Dyads: Competitive Electron Transfer versus Intersystem Crossing upon Photoexcitation. *ChemPhotoChem* **2020**, *4*, 68–81.

(76) Zhao, J.; Xu, K.; Yang, W.; Wang, Z.; Zhong, F. The Triplet Excited State of Bodipy: Formation, Modulation and Application. *Chem. Soc. Rev.* **2015**, *44*, 8904–8939.

(77) Snellenburg, J.; Laptenok, S.; Seger, R.; Mullen, K.; van Stokkum, I. Glotaran: A Java-Based Graphical User Interface for the R Package TIMP. *J. of Stat. Softw.* **2012**, 49, 1-22.

(78) http://glotaran.org/index.html.

(79) Marcus, R. A. Electron Transfer Reactions in Chemistry: Theory and Experiment (Nobel Lecture). *Angew. Chem. Int. Ed. Engl.* **1993**, *32*, 1111–1121.

Table of content